

A High Efficient DC-DC Converter with Soft Switching for Stress Reduction

S.K.Anuja, R.Satheesh Kumar
 M.E. Student, M.E. Lecturer
 Sona College of Technology
 Salem, TamilNadu, India

ABSTRACT

Soft switching of DC-DC converter is done here. This is obtain good efficiency and to reduce the switching losses. Zero voltage switching reduces the switching losses in the circuit. This is done by using boost converter. Soft-switching characteristic of the proposed converter reduces switching loss of active power switches and raises the conversion efficiency. A voltage step-up function and a continuous input current, a continuous-conduction-mode (CCM) boost converter is used to produce continuous input current and is simple. This method also provides high voltage gain.

Keywords:

Soft switching, boost converter, high efficiency, high voltage gain

1. INTRODUCTION

Now-a-days energy requirement has increased to a great extent which has to be met. Thus the power systems based on battery sources and super-capacitors have been increased [1],[2]. Unfortunately, the output voltages of these sources are relatively low. Therefore, the step-up power conversion is required in these systems. More demands are rising in the case of efficiency, dynamics, weight being light etc. Besides the step-up function, the demands such as low current ripple, high efficiency, fast dynamics, light weight, etc. [3],[4]. One of the major trends in power electronics is increasing the switching frequencies. The faster semiconductors working at high frequencies result in the passive components of the converters – capacitors, inductors and transformers – becoming smaller thereby reducing the total size and weight of the equipment and hence to increase the power density.[5] Novel soft-switching converters combine the functions of loss-less soft- switching for all switches and secondary output voltage regulation at constant switching frequency.

This was made possible by using magnetic amplifiers in series with the rectifier diodes in the symmetrical topologies. The primary side switches are driven at constant frequency and near 50% [6] duty ratio with small dead-time and the output voltage is regulated. The DC-DC converter finds wider usage in not only electrical field, but also in all other resources. In most of the cases the DC-DC converter utilizes a multilinking coupled inductor and a voltage doubler to achieve high step-up voltage gain.

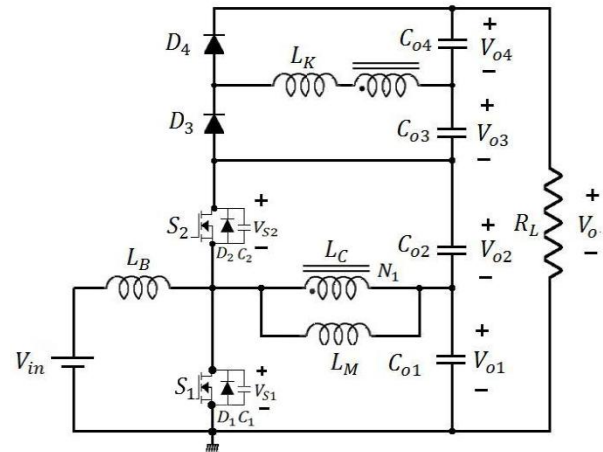


Fig:1 Diagram of the Proposed converter

The voltage on the active switch is clamped, and the energy stored in the leakage inductor is recycled [7]. Therefore, the voltage stress on the active switch is reduced, and the conversion efficiency is improved [8]. In fuel cell it is used [9]-[13]. However, the conversion efficiency and the step-up voltage gain are limited due to the constraints of the losses of power switches and diodes.[14]-[19]. High step-up converters with a low input current ripple based on the coupled inductor have been developed [20],[21]. A soft-switching dc/dc converter with high voltage gain is shown in the Fig.1. A CCM boost cell provides a continuous input current. To increase the voltage gain, the output of the coupled inductor cell is laid on the top of the output of CCM boost cell. Therefore, the high voltage gain is obtained without high turn ratio of the coupled inductor, and the voltage stresses of the switches are confined to the output voltage of the CCM boost cell. A zero-voltage-switching (ZVS) operation of the converter reduces the switching losses during transition and thus improves the overall efficiency.

2. CONVERTER OPERATING MODES

Fig. 1 shows the circuit diagram of the proposed soft-switching dc/dc converter with high voltage gain. C_1 and C_2 are the parasitic output capacitances of S_1 and S_2 . The proposed converter contains a CCM boost cell. The CCM boost cell provides a continuous input current. When the switch is turned on, the boost inductor current increases linearly from its minimum value to its maximum value. To obtain ZVS of S_1 and S_2 and high voltage gain, a coupled inductor L_c is inserted.

The coupled inductor L_c is modeled as the magnetizing inductance L_m , the leakage inductance L_k , and the ideal transformer that has a turn ratio of $1:n$ ($n = N_2/N_1$).

2.1 Continuous Mode

When a boost converter operates in continuous mode, the current through the inductor (I_L) never falls to zero. Figure below shows the typical waveforms of currents and voltages in a converter operating in this mode. The output voltage can be calculated as follows, in the case of an ideal converter (i.e. using components with an ideal behavior) operating in steady conditions.

During the On-state, the switch S is closed, which makes the input voltage (V_i) appear across the inductor, which causes a change in current (I_L) flowing through the inductor during a time period (t) by the formula:

$$\frac{\Delta I_L}{\Delta t} = \frac{V_i}{L} \quad (1)$$

At the end of the On-state, the increase of I_L is therefore:

$$\Delta I_{L_{on}} = \frac{1}{L} \int_0^{DT} V_i dt = \frac{DT}{L} V_i \quad (2)$$

D is the duty cycle. It represents the fraction of the commutation period T during which the switch is On. Therefore D ranges between 0 (S is never on) and 1 (S is always on).

During the Off-state, the switch S is open, so the inductor current flows through the load. If we consider zero voltage drop in the diode, and a capacitor large enough for its voltage to remain constant, the evolution of I_L is:

$$V_i - V_o = L \frac{dI_L}{dt} \quad (3)$$

Therefore, the variation of I_L during the Off-period is:

$$\Delta I_{L_{off}} = \int_0^{(1-D)T} \frac{(V_i - V_o) dt}{L} = \frac{(V_i - V_o)(1-D)T}{L} \quad (4)$$

As we consider that the converter operates in steady-state conditions, the amount of energy stored in each of its components has to be the same at the beginning and at the end of a commutation cycle. In particular, the energy stored in the inductor is given by:

$$E = \frac{1}{2} L I_L^2 \quad (5)$$

So, the inductor current has to be the same at the start and end of the commutation cycle. This means the overall change in the current (the sum of the changes) is zero:

$$\Delta I_{L_{on}} + \Delta I_{L_{off}} = 0 \quad (6)$$

Substituting $\Delta I_{L_{on}}$ and $\Delta I_{L_{off}}$ by their expressions yields:

$$\Delta I_{L_{on}} + \Delta I_{L_{off}} = \frac{V_i DT}{L} + \frac{(V_i - V_o)(1-D)T}{L} = 0 \quad (7)$$

This can be written as:

$$\frac{V_o}{V_i} = \frac{1}{1-D} \quad (8)$$

This in turn reveals the duty cycle to be:

$$D = 1 - \frac{V_i}{V_o} \quad (9)$$

From the above expression it can be seen that the output voltage is always higher than the input voltage (as the duty cycle goes from 0 to 1), and that it increases with D, theoretically to infinity as D approaches 1. This is why this converter is sometimes referred to as a step-up converter.

2.2 Discontinuous Mode

In some cases, the amount of energy required by the load is small enough to be transferred in a time smaller than the whole commutation period. In this case, the current through the inductor falls to zero during part of the period. The only difference in the principle described above is that the inductor is completely discharged at the end of the commutation cycle (see waveforms in figure 4). Although slight, the difference has a strong effect on the output voltage equation. It can be calculated as follows:

As the inductor current at the beginning of the cycle is zero, its maximum value $I_{L_{max}}$ (at $t = DT$) is

$$I_{L_{max}} = \frac{V_i DT}{L} \quad (10)$$

During the off-period, I_L falls to zero after δT :

$$I_{L_{max}} + \frac{(V_i - V_o)\delta T}{L} = 0 \quad (11)$$

Using the two previous equations, δ is

$$\delta = \frac{V_i D}{V_o - V_i} \quad (12)$$

The load current I_o is equal to the average diode current (I_D). As can be seen on figure the diode current is equal to the inductor current during the off-state. Therefore the output current can be written as

$$I_o = I_D = \frac{I_{L_{max}}}{2} \delta \quad (13)$$

Replacing $I_{L_{max}}$ and δ by their respective expressions yields

$$I_o = \frac{V_i DT}{DT} \cdot \frac{V_i D}{V_o - V_i} = \frac{V_i^2 D^2 T}{2L(V_o - V_i)} \quad (14)$$

Therefore, the output voltage gain can be written as follow

$$\frac{V_o}{V_i} = 1 + \frac{V_i D^2 T}{2L(V_o - V_i)} \quad (15)$$

Compared to the expression of the output voltage for the continuous mode, this expression is much more complicated. Furthermore, in discontinuous operation, the output voltage gain not only depends on the duty cycle, but also on the inductor value, the input voltage, the switching frequency, and the output current.

3. BASIC BLOCK DIAGRAM OF SOFT-SWITCHING OF CONVERTER

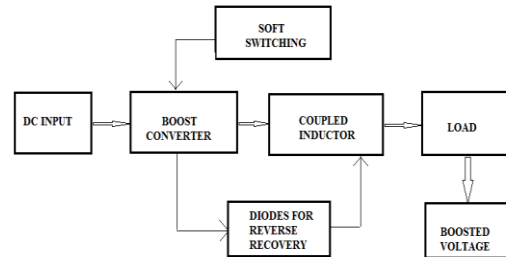


Fig.2. Block Diagram for soft-switching of the DC-DC converter

4. ANALYSIS OF THE CONVERTER

Various operating modes are performed for this converter operation. The voltage doublers consists of diodes D1, D2 and the output capacitors C_{o3} , C_{o4} , and the secondary winding N_2 of the coupled inductor L_c is on the top of the output stage of the boost cell to increase voltage gain.

$$V_{o1} = V_{in} \quad (16)$$

$$V_{o2} = \frac{D}{1-D} V_{in} \quad (17)$$

Mode 1 [t_0, t_1]: At t_0 Switch S2 is switched off. Before t_0 switch S2 and diode D4 are conducting. Therefore the voltage across S1 starts to fall and the voltage across S2 starts to rise. The capacitance output is very small. The transition interval is short and it is neglected. So the inductor currents will have constant values during this mode.

$$T_{t1} = \frac{(C_1 + C_2)V_{in}}{(1-D)(L_{L1} + L_{LB2})} \quad (18)$$

Mode 2 [t_1, t_2]: At t_1 the voltage across S1 will become Zero and the diode D1 is turned on. Hence the switch S1 will receive the gate signal. Diode D1 receives the current which is flowing already and the voltage becomes zero before S1 is turned on. Here zero-voltage switching is achieved. The magnetizing current i_m , the primary current i_1 , the secondary current i_2 , and the inductor current i_L are obtained.

$$I_m(t) = I_{m1} - V_{in} L_m (t - t_1) \quad (19)$$

Mode 3 [t_2, t_3]: During t_2 the secondary current changes its direction. The current from diode D4 decreases to zero and the diode D4 is turned off. At this time the diode D3 is turned on and the current through diode D3 increases linearly. The current changing rate of D4 is controlled by the leakage inductance of the coupled inductor. Hence the reverse recovery problem is alleviated.

$$I_m(t) = I_m(t_2) - V_{in} L_m (t - t_2) \quad (20)$$

Mode 4 [t_3, t_4]: During time t_3 , switch S1 is turned off. Hence the boost inductor current and the coupled inductor current starts to charge capacitor C1 and discharge C2. Hence the voltage rise and fall in this mode is similar to that of mode 1. Hence the inductor currents will have constant values.

$$T_{t1} = \frac{(C_1 + C_2)V_{in}}{(1-D)(L_{L2} + L_{LB2})} \quad (21)$$

Mode 5 [t_4, t_5]: During t_4 the voltage across S2 becomes zero and the diode D2 will be turned on. Hence switch S2 will receive the gate signal. Since the current has already flown through the diode D2 and the voltage becomes zero before the switch S2 is achieved. The boost inductor current decreases linearly.

$$I_m(t) = -I_{m2} + DV_{in} L_m (1 - D)(t - t_4) \quad (22)$$

Mode 6 [t_5, t_6]: During this mode at t_5 , the secondary current will change its direction. The current through the diode D3 decreases to zero and D3 is turned off. Hence the reverse recovery problem is alleviated.

The volt-second break law gives

$$V_{in} D T_s - (V_{o1} + V_{o2} - V_{in})(1 - D) T_s = 0 \quad (23)$$

The output current from the converter is given by

$$I_o = \frac{(D - \Delta_1 + \Delta_2) I_{D3}}{2} \quad (24)$$

$$= \frac{(1 - D + \Delta_1 - \Delta_2) I_{D4}}{2} \quad (25)$$

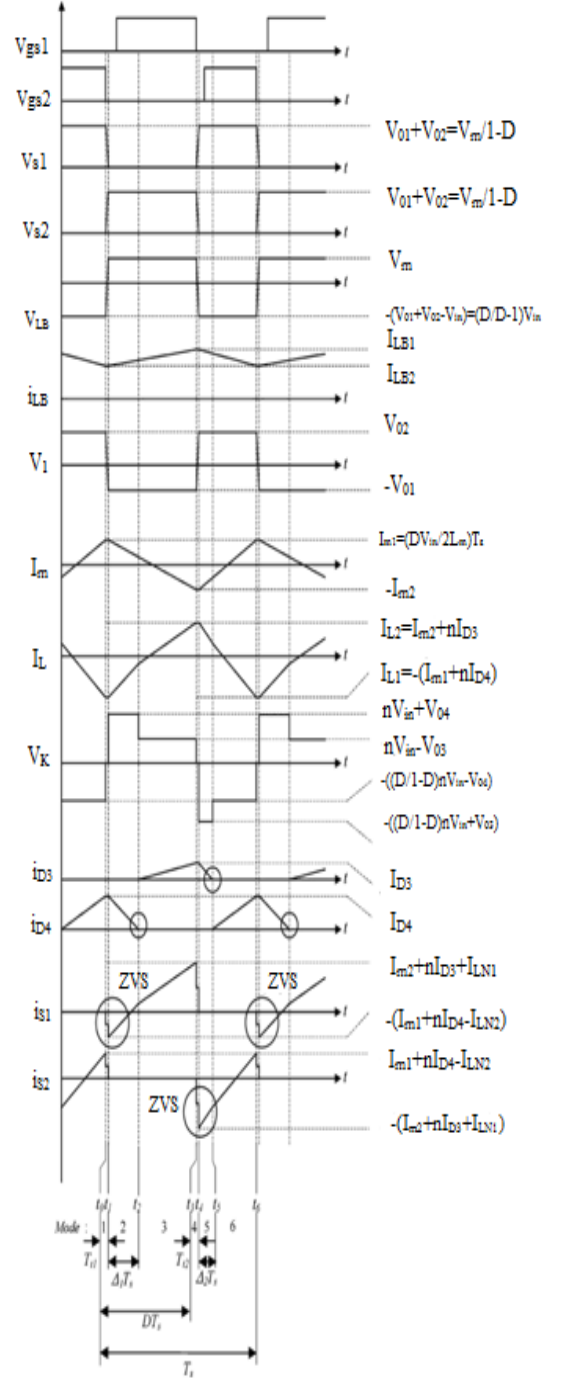


Fig.3. Waveforms of the converter

Where I_{D3} and I_{D4} are given by

$$I_{D3} = \frac{V_{in} - V_{o3}}{L_k} (D - \Delta_1) T_s \quad (26)$$

$$I_{D4} = \frac{V_{in} + V_{o4}}{L_k} \Delta_1 T_s \quad (27)$$

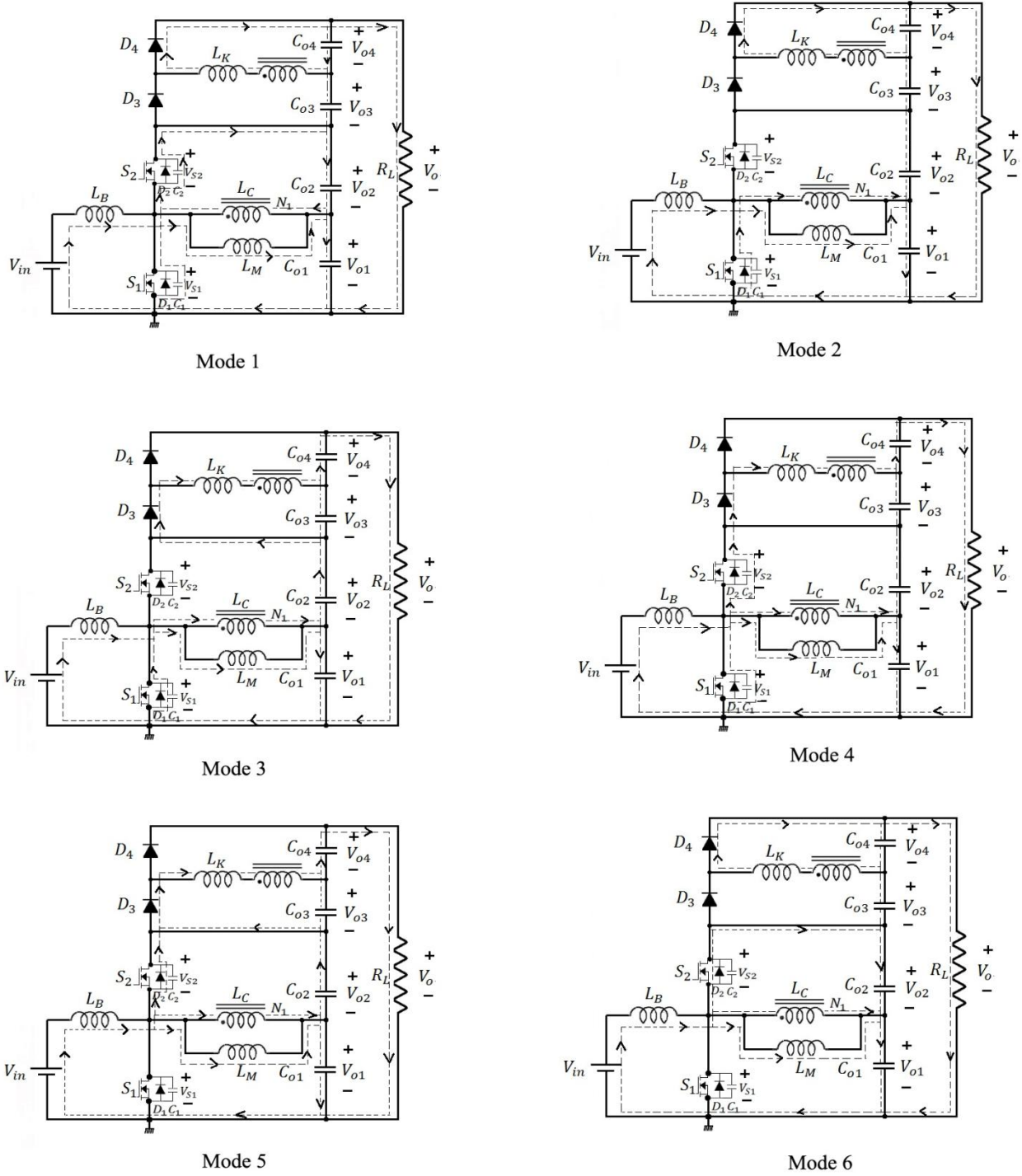


Fig.4. Converter operating modes.

5. CHARACTERISTIC AND DESIGN PARAMETERS

5.1. Input Current Ripple

The input current ripple is given by

$$\Delta I_{LB} = I_{LB1} - I_{LB2} = \frac{DV_{in}T_s}{L_B} \quad (28)$$

To reduce the input current ripple below a specific value, the inductor should satisfy the following

$$L_B > \frac{DV_{in}T_s}{I} \quad (29)$$

5.2. Voltage Gain

The voltage gain of the converter is given by

$$\frac{V_{in}}{V_{in}} = \frac{1}{1-D} + \frac{nD(1-\alpha)}{(D-\alpha(2D-1))(1-D+\alpha(2D-1))} \quad (30)$$

As α increases, the voltage gain decreases. Larger value of Inductor decreases the gain.

5.3. Voltage Stress of Devices

Generally, high output voltage will impose high-voltage stress across the switching devices in dc/dc converters. In the proposed dc/dc converter, the voltage stresses across the switching devices are smaller than the output voltage. Maximum values of voltage across switch S1 and S2 are confined to the output of the CCM boost cell as follows:

$$V_{S1max} = V_{S2max} = V_{O1} + V_{O2} = \frac{V_{in}}{1-D} \quad (31)$$

The maximum voltage stress across the diodes are given by the following

$$V_{D1max} = V_{D2max} = V_{O3} + V_{O4} = V_o - \frac{V_{in}}{1-D} \quad (32)$$

6. EXPERIMENTAL RESULTS

The soft-switching of a DC/DC converter is implemented with high voltage specifications. The input voltage is given as $V_{in}=24V$. The boosted output voltage obtained is 360V. Fig 5 shows experimental result output. It can be seen from the results that the experimental output agrees with the theoretical output. The input current is continuous and the ripple is controlled by the inductor. It also shows that the reverse recovery current is reduced and the reverse recovery problem is alleviated by the leakage inductor.

The Fig.6. Shows measured efficiency of the converter. The efficiency is about 96.4% at full load. Due to soft-switching the reverse recovery problem is alleviated and the efficiency is improved by 2% when compared with the conventional step-up booster.

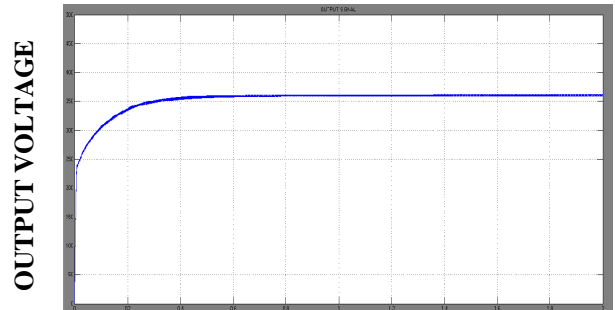


Fig.5. Experimental Output waveform

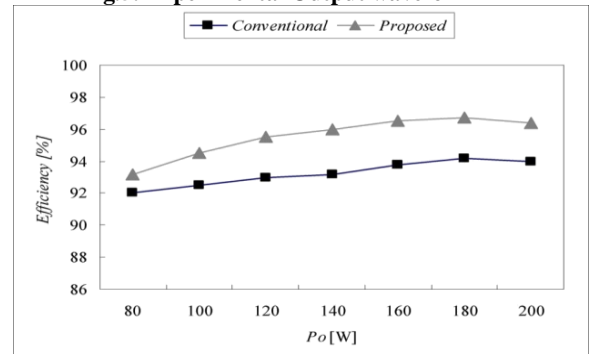


Fig.6. Measured efficiency output

7. CONCLUSION

A soft-switching converter is proposed in this paper which reduces stresses and improves the efficiency. It gives a continuous input current so that gain is increased. This continuous input current is given by the CCM boost converter. Soft-switching improves the overall efficiency and alleviates the reverse recovery problem with the help of leakage inductor.

8. REFERENCES

- [1] F. Blaabjerg, Z. Chen, and S. B. Kjaer, "Power electronics as efficient interface in dispersed power generation systems," *IEEE Trans. Power Electron.*, vol. 19, no. 5, pp. 1184–1194, Sep. 2004.
- [2] R. J. Wai, W. H. Wang, and C. Y. Lin, "High-performance stand-alone photovoltaic generation system," *IEEE Trans. Ind. Electron.*, vol. 55, no. 1, pp. 240–250, Jan. 2008.
- [3] C. Wang, Y. Kang, B. Lu, J. Sun, M. Xu, W. Dong, F. C. Lee, and W. C. Tipton, "A high power-density, high efficiency front-end converter for capacitor charging application," in *Proc. IEEE APEC*, Mar. 2005, vol. 2, pp. 1258–1264.
- [4] Z. Qun and F. C. Lee, "High-efficiency, high step-up DC–DC converters," *IEEE Trans. Power Electron.*, vol. 18, no. 1, pp. 65–73, Jan. 2003.
- [5] K. Kobayashi, H. Matsuo, and Y. Sekine, "Novel

- solar-cell power supply system using a multiple-input DC–DC converter,” *IEEE Trans. Ind. Electron.*, vol. 53, no. 1, pp. 281–286, Feb. 2006
- [6] Tsai-Fu Wu, Yung-Chu Chen, Jeng-Gung Yang, Chia-Ling Kuo, “Isolated Bidirectional Full bridge DC-DC Converter with a Flyback Snubber” *IEEE Trans. Power Electron.*, vol. 25, no. 7, pp. 1915–1922, July 2010.
- [7] R. Watson, F.C. Lee and G. C. Hua, “Utilization of an active-clamp circuit to achieve soft switching in Flyback converters”, *Power Electronics Specialist Conference*, 1994, pp. 909–916.
- [8] J. P. Rodrigues, S. A. Mussa, M. L. Heldwein, and A. J. Perin, “Three level ZVS active clamping PWM for the DC–DC buck converter,” *IEEE Trans. Power Electron.*, vol. 24, no. 10, pp. 2249–2258, Oct. 2009.
- [9] S. J. Jang, C. Y. Won, B. K. Lee, and J. Hur, “Fuel cell generation system with a new active clamping current-fed half-bridge converter,” *IEEE Trans. Energy Convers.*, vol. 22, no. 2, pp. 332–340, Jun. 2007.
- [10] J. M. Correa, F. A. Farret, N. Canha, and M. G. Simoes, “An electrochemical-based fuel-cell model suitable for electrical engineering automation approach,” *IEEE Trans. Ind. Electron.*, vol. 51, no. 5, pp. 1103–1112, Oct. 2004.
- [11] Z. Jiang and R. A. Dougal, “A compact digitally controlled fuel cell/battery hybrid power source,” *IEEE Trans. Ind. Electron.*, vol. 53, no. 4, pp. 1094–1104, Aug. 2006.
- [12] S. M. Lukic, J. Cao, R. C. Bansal, F. Rodriguez, and A. Emadi, “Energy storage systems for automotive applications,” *IEEE Trans. Ind. Electron.*, vol. 55, no. 6, pp. 2258–2267, Jun. 2008.
- [13] H. Tao, J. L. Duarte, and A.M. Hendrix, “Line-interactive UPS using a fuel cell as the primary source,” *IEEE Trans. Ind. Electron.*, vol. 55, no. 8, pp. 3012–3021, Aug. 2008.
- [14] R. Huang and S. K. Mazumder, “A soft-switching scheme for an isolated DC/DC converter with pulsating DC output for a three-phase high frequency-link PWM converter,” *IEEE Trans. Power Electron.*, vol. 24, no. 10, pp. 2276–2288, Oct. 2009
- [15] S. J. Finney, B. W. Williams, and T. C. Green, “RCD snubber revisited,” *IEEE Trans. Ind. Appl.*, vol. 32, no. 1, pp. 155–160, Jan./Feb. 1996.
- [16] D. D. C. Lu, D. K. W. Cheng, and Y. S. Lee, “A single-switch continuous conduction-mode boost converter with reduced reverse-recovery and switching losses,” *IEEE Trans. Ind. Electron.*, vol. 50, no. 4, pp. 767–776, Aug. 2003.
- [17] Y. S. Lee and B. T. Lin, “Adding active clamping and soft switching to boost–flyback single-stage isolated power-factor-corrected power supplies,” *IEEE Trans. Power Electron.*, vol. 12, no. 6, pp. 1017–1027, Nov. 1997.
- [18] C. M. C. Duarte and I. Barbi, “An improved family of ZVS-PWM active clamping DC-to-DC converters,” *IEEE Trans. Power Electron.*, vol. 17, no. 1, pp. 1–7, Jan. 2002.
- [19] T. F. Wu, Y. S. Lai, J. C. Hung, and Y. M. Chen, “Boost converter with coupled inductors and buck–boost type active clamp,” *IEEE Trans. Ind. Electron.*, vol. 55, no. 1, pp. 154–162, Jan. 2008.
- [20] W. Cheng, X. C. Liu, and Y. S. Lee, “A new improved boost converter with ripple free input current using coupled inductors,” in *Proc. IEE Int. Conf. Power Electron. Variable Speed Drives*, London, U.K., 1998, pp. 592–599.
- [21] J. Wang, W. G. Dunford, and K. Monrad, “Analysis of a ripple-free input current boost converter with discontinuous conduction characteristics,” *IEEE Trans. Power Electron.*, vol. 12, no. 4, pp. 684–694, Jul. 1997.